The miR-625-3p/*AXL* axis induces non-T790M acquired resistance to EGFR-TKI via activation of the TGF-β/Smad pathway and EMT in EGFR-mutant non-small cell lung cancer

WENWEN DU[1,2*], LIN SUN[1,2*], TING LIU[1,2*], JIANJIE ZHU[1-3], YUANYUAN ZENG[1-3], YANG ZHANG[1,2], XUETING WANG[1,2], ZEYI LIU[1-3] and JIAN-AN HUANG[1-3]

[1]Department of Respiratory Medicine, The First Affiliated Hospital of Soochow University; [2]Suzhou Key Laboratory for Respiratory Diseases; [3]Institute of Respiratory Diseases, Soochow University, Suzhou, Jiangsu 215006, P.R. China

Received December 28, 2019; Accepted March 20, 2020

DOI: 10.3892/or.2020.7579

Abstract. Gefitinib is currently the preferred treatment for non-small cell lung cancer (NSCLC) patients with epidermal growth factor receptor (*EGFR*)-activating mutation. However, some patients gradually develop acquired resistance after receiving treatment. In addition to secondary T790M mutation, the remaining mechanisms contributing to non-T790M mutations need to be explored. In the present study, NSCLC-derived HCC827 and PC-9 cells and the corresponding gefitinib-resistant cell lines (HCC827GR and PC9GR) were utilized. Next-generation DNA sequencing was performed on the HCC827GR and PC9GR cells. Under AXL receptor tyrosine kinase (*AXL*) knockdown or miR-625-3p overexpressing conditions, a cell growth inhibition assay was performed to evaluate gefitinib sensitivity. Wound healing and Transwell assays were used to examine the migratory and invasive abilities of the cells. Moreover, we also carried out western blot analysis to detect the altered downstream signaling pathway. Our study revealed markedly decreased miR-625-3p expression in the HCC827GR cell line, while its overexpression partly reversed gefitinib resistance. Integrated analysis based on Targetscan website showed that *AXL* can be potentially targeted by miR-625-3p and we further verified the hypothesis via dual-luciferase reporter assays. Mechanistic analysis revealed that TGF-β1-induced EMT may contribute to the miR-625-3p/*AXL* axis-mediated gefitinib resistance. Our data demonstrated that miR-625-3p contributes to the acquired resistance of gefitinib, which may provide novel insight to combat resistance to EGFR-TKIs.

Correspondence to: Professor Zeyi Liu or Professor Jian-An Huang, Department of Respiratory Medicine, The First Affiliated Hospital of Soochow University, 899 Pinghai Road, Suzhou, Jiangsu 215006, P.R. China
E-mail: liuzeyisuda@163.com
E-mail: huang_jian_an@163.com

*Contributed equally

Abbreviations: NSCLC, non-small cell lung cancer; TGF-β1, transforming growth factor-β1; HCC827GR, HCC827 gefitinib resistant; EGFR-TKIs, epidermal growth factor receptor-tyrosine kinase inhibitors; EMT, epithelial to mesenchymal transition

Key words: miR-625-3p, non-small cell lung cancer, gefitinib acquired resistance, *AXL*, EMT

Introduction

Lung cancer is the leading cause of cancer-related death worldwide, and approximately 85% of all diagnosed lung cancer cases are non-small cell lung cancer (NSCLC) (1,2). Great progress in therapeutic strategies has been made over the past decades including the discovery of epidermal growth factor receptor (EGFR)-tyrosine kinase inhibitors (TKIs), which have dramatically changed the prognosis of advanced NSCLC patients harboring specific *EGFR*-activating mutations (3,4). However, patients who initially respond to EGFR-TKIs eventually acquire resistance, resulting in progression and relapse (5,6). Several mechanisms are believed to be responsible for acquired EGFR-TKI resistance. The secondary *EGFR* T790M mutation that can eliminate inhibition of the respective TKIs accounts for half of the potential mechanisms (7). The remaining resistance mechanisms under non-T790M mutation status can be classified into three types. Phenotypic or histological changes include small cell lung cancer (SCLC) transformation and epithelial to mesenchymal transition (EMT) process. Accumulating studies point to a molecular association between EMT and TKI resistance. Tissue samples of lung cancer patients who develop acquired resistance to erlotinib were found to consist of EMT features (8). Activation of AXL receptor tyrosine kinase (*AXL*) and transforming growth factor-β (TGF-β) is associated with the EMT process in EGFR-TKI-resistant NSCLC (9). In terms of compensatory bypass signaling pathways, insulin-like growth factor 1 receptor (IGF1R)/MEK, *AXL*/PI3K/AKT, hepatocyte growth factor receptor (HGFR)/MAPK pathways were found to be involved in TKI resistance (10). It has been reported that the InsR/IGF1R pathway confers resistance to gefitnib resistance in glioblastoma through AKT regulation (11). Point mutations

of target genes also contribute to non-T790M mutations such as *HER2* amplification, *MET* amplification, *BRAF* mutation and *PIK3CA* mutation (12). Osimertinib is a third-generation EGFR-TKI used for the treatment of patients with the T790M mutation; however no special treatment has been discovered for patients harboring non-T790M mutations (13,14). Therefore, further elucidation of other potential mechanisms that are critical for the development of effective therapeutic strategies targeting patients without the T790M mutation is urgent.

MicroRNAs are a class of small non-coding RNAs that play essential roles in tumor development and progression via the regulation of various networks that are associated with multiple cellular functions, such as proliferation, migration, and metabolism (15). Accumulating evidence has shown that a number of microRNAs may have a specific role in lung cancer pathogenesis and biological and pathological behaviors as well as in modulating the response to anticancer treatments, particularly EGFR-TKIs (16,17). It is reported that circulating miR-21 expression in the peripheral blood of patients significantly increased from the baseline to high levels with the progression of disease following treatment with EGFR-TKI. Mechanically, miR-21 was found to induce EGFR-TKI resistance via downregulating *PTEN* and *PDCD4* and activating the PI3K/AKT pathway (18). MicroRNAs have also been reported to reverse drug resistance in addition to contributing to gefitinib resistance in tumor cells. miR-506-3p was identified to reverse gefitinib resistance by targeting Yes-associated protein 1 in the PC9GR cell line (19). miR-497 was reported to enhance the sensitivity of NSCLC cells to gefitinib by targeting *IGFR-1* (20).

In the present study, we mainly focused on the identification of new microRNAs underlying non-T790M mutation-induced gefitinib resistance. Here, we found that the PC9GR cell line acquired a secondary T790M mutation, herein the non-T790M mutated HCC827GR cell line was selected for our experiments. Our results showed that miRNA-625-3p was significantly downregulated in HCC827GR cells compared to that noted in the HCC827 cells. Overexpression of miRNA-625-3p was found to enhance sensitivity to gefitinib and inhibit the migratory and invasive abilities of HCC827GR cells. Furthermore, a functional assay also indicated that miRNA-625-3p could directly target *AXL* to reverse the EMT process. Taken together, these results suggest that the modulation of miRNA-625-3p may be a potential strategy to overcome gefitinib acquired resistance in NSCLC.

Materials and methods

Cell culture and reagents. The NSCLC cell line HCC827 and 293T cells were purchased from the Cell Bank of the Chinese Academy of Sciences (Shanghai, China). To establish the gefitinib-resistant cell strain HCC827GR, HCC827 cells were exposed to gefitinib as previously described (21). The NSCLC cell line PC9 and PC9 gefitinib-resistant (PC9GR) cell line were obtained from Professor Caicun Zhou (Shanghai Pulmonary Hospital) as a gift and were maintained in Dulbecco's modified Eagle's medium (DMEM; Gibco, Carlsbad, CA, USA) supplemented with 10% foetal bovine serum (FBS) (Gibco; Thermo Fisher Scientific, Inc.) and 1% penicillin/streptomycin (Gibco; Thermo Fisher Scientific, Inc.). All cell lines were cultured at 37˚C in a humidified atmosphere containing 5% CO_2. Among all cell lines, both HCC827 and PC9 cell lines contain exon 19 deletions (del 19). PC9GR cells contain the T790M mutation while HCC827 do not. Detailed mutation information is documented in Table SII. The EGFR inhibitor gefitinib was purchased from Selleck, at doses of 0-40 μM (Selleck Chemicals).

Next-generation DNA sequencing. The DNAseq was performed by Geneseeq Co. DNA from cell lines was profiled and then analyzed using a capture-based targeted sequencing panel. Human genomic regions totalling 1.4 megabases in size, including selected exons and introns of 357 genes, were captured using 120-bp probes. DNA was fragmented into segments 200 to 250 bp in length, captured by the 120-bp probes, and sequenced by obtaining paired 2x150-bp reads. After DNA extraction with the QIAamp DNA Mini Kit (Qiagen), DNA concentrations were measured using the Qubit dsDNA assay (Invitrogen; Thermo Fisher Scientific, Inc.). The DNA quality was confirmed by checking that the A260/A280 ratio was 1.8:2.0. The appropriate concentration value for samples was higher than 100 ng/μl and 4 mg DNA was needed for each sample. DNA was hybridized with the capture probes (the bait), selected using magnetic beads, and polymerase chain reaction (PCR)-amplified. Then, a Qubit and Agilent 2100 bioanalyzer (Agilent Technologies) was used to perform high-sensitivity assays assessing DNA quality and size range. All samples were sequenced on a HiSeq 4000 platform (Illumina, Inc.) and pair-end reads were obtained. For tissue samples, we aimed to achieve an average sequencing depth of 2,000x for all targeted regions.

miRNA library construction and RNA sequencing

Sample preparation. Total RNA was extracted from HCC827 and HCC827GR cells by TRIzol reagent (Invitrogen; Thermo Fisher Scientific, Inc.) separately. The RNA quality was checked by a Bioanalyzer 2200 (Agilent Technologies) and stored at -80˚C. RNA with RNA integrity number (RIN) >6.0 was appropriate for miRNA purification. miRNA was purified by the miRNeasy Mini Kit (Qiagen), and the purity was validated by gel electrophoresis.

The complementary DNA (cDNA) libraries for single-end sequencing were prepared using the Ion Total RNA-Seq Kit v2.0 (Life Technologies; Thermo Fisher Scientific, Inc.) according to the manufacturer's instructions. The cDNA library was size selected by PAGE gel electrophoresis for miRNA sequencing. The cDNA libraries were then processed for the proton sequencing process according to commercially available protocols. Samples were diluted and mixed, and the mixture was processed on a OneTouch 2 Instrument (Life Technologies; Thermo Fisher Scientific, Inc.) and enriched on a OneTouch 2 ES station (Life Technologies; Thermo Fisher Scientific, Inc.) to prepare the template-positive Ion PI™ Ion Sphere™ Particles (Life Technologies; Thermo Fisher Scientific, Inc.) according to the instructions for the Ion PI™ Hi-Q OT2 200 Kit (Life Technologies; Thermo Fisher Scientific, Inc.). After enrichment, the mixed template-positive Ion PI™ Ion Sphere™ Particles of the samples were loaded onto 1 v3 Proton Chip (Life Technologies; Thermo Fisher Scientific, Inc.) and sequenced on Proton Sequencers according

to the protocol for the Ion PI Hi-Q Sequencing 200 Kit (Life Technologies; Thermo Fisher Scientific, Inc.) by NovelBio Corp. Laboratory, Shanghai.

Filtering and miRNA mapping. We performed filtering of the raw reads after sequencing to obtain clean data using the following criteria: i) 30% base quality <20, ii) the sequences shorter than 15 bp or longer than 33 bp were discarded, and iii) presence of the adaptor sequence. Utilizing the BWA software BSA-backtrack) (22), we mapped the clean data to the human miRNA database (miRBase v21.0) (23) and the human genome (GRCh38, NCBI) (24).

RNA sequencing mapping/mapping of pair-end reads. Before read mapping, clean reads were obtained from the raw reads by removing the adaptor sequences, reads with >5% ambiguous bases (noted as N) and low-quality reads containing more than 20% of bases with quality of <20. The clean reads were then aligned to the human genome (version: GRCh38) using the HISAT2 programme (25). Dif-Gene-Finder (26) and Target Analysis were described in our previous study (27).

Cell transfection. Transient transfection of miR-625-3p mimics, miR-NC, control siRNA and *AXL* siRNA was carried out using Lipofectamine 2000 Reagent (Invitrogen; Thermo Fisher Scientific, Inc.) according to the manufacturer's protocols. The target siRNA sequences are: si-NC, 5'-UUCUCCGAACGU GUCACGUTT-3'; si-*AXL*: 5'-ACAGCGAGAUUUAUGACU ATT-3'. The sequences of miR-625-3p are as follows: Sense, GACUAUAGAACUUUCCCCCUCA and antisense, UGA GGGGGAAAGUUCUAUAGUC; for miR-NC, sense, UUU GUACUACACAAAAGUACUG and antisense, CAGUAC UUUUGUGUAGUACAAA. All mimics were synthesized by Guangzhou Ribo BioCompany (Guangzhou, China). siRNAs were provided by GenePharma Co. Cells were plated in 6-well plates ($2x10^5$ cells/well) in advance. At 50% confluence, the cells were transfected with 0.1 nmol miR-625-3p mimics, miR-NC or 100 pmol siRNAs using Lipofectamine 2000 transfection reagent in medium without serum. After 6 h, the medium was changed to RPMI-1640 supplemented with 10% FBS. After 48 h, the cells were collected for subsequent experiments.

Cell growth inhibition assay. After transfection with miR-625-3p mimics, miR-NC or siRNAs, the cells were seeded in 96-well plates ($3x10^3$ cells/well) overnight. Gefitinib was added in a dose-dependent manner, and the cells were incubated for 72 h. Then, we used the Cell Counting Kit-8 assay kit (CCK-8, Boster) to assess cell proliferation according to the manufacturer's instructions. Each sample was plated in triplicate, and three independent experiments were performed. The half maximal inhibitory concentration (IC_{50}) was defined as the concentration needed for a 50% reduction in the absorbance.

Wound healing assay. The wound healing assay was used to determine the cell migration ability. After cells formed a monolayer in 6-well plates, cells were washed with PBS and then cultured in RPMI-1640 medium with 1% FBS overnight. Then the wound assay was performed. A straight scratch was made gently through the cell monolayer using a 10-μl pipette tip. Detached cells were washed away with PBS, and then fresh RPMI-1640 medium with 10% FBS was added. The cells were imaged at 0 and 24 h after wounding using a light microscope (CKX41; Olympus, magnification, x100).

Transwell assays. For the migration assay, 800 μl medium supplemented with 10% FBS was added to the lower well, and $4x10^4$ cells in 200 μl medium supplemented with 1% FBS were seeded into the upper chamber of a Transwell insert. The cells were incubated for 24 h at 37˚C in 5% CO_2. For the invasion assay, the inserts were coated with a Matrigel matrix (BD Science), which was diluted in serum-free medium and incubated at 37˚C for 2 h before cell plating. In both assays, the cells were then imaged under a light microscope (IX73; Olympus). The detailed cell numbers in each field were counted via ImageJ software (National Institutes of Health). Three independent experiments were performed.

Plasmid construction and dual-luciferase reporter assay. To construct a plasmid containing the *AXL* 3'-UTR (3' untranslated region) fused to the 3' end of a luciferase reporter, a 221-bp fragment containing the predicted miR-625-3p target site (positions 905-911) was inserted into the psiCHECK-2 dual-luciferase vector (Promega). The potential binding sites were predicted by TargetScan (http://www.targetscan.org/). The psiCHECK-2-*AXL*-3'-UTR wild-type and mutated fragments were synthesized and subcloned directly (Genewiz). Cells were plated in a 24-well plate overnight and then co-transfected with the wild-type or mutated plasmid, control pRL-TK plasmid and with either miR-625-3p mimics or miR-NC using Lipofectamine 2000 (Life Technologies; Thermo Fisher Scientific, Inc.). Then, the cells were harvested, and luciferase activities were evaluated using a Dual-Luciferase Reporter Assay Kit (Promega). Each experiment was performed in triplicate.

RNA isolation and RT-qPCR. Trizol reagent was used to extract RNA (Takara). In our study, we extracted RNA from HCC827 and HCC827GR cells to detect miR-625-3p and *AXL* mRNA expression to verify the sequencing results. After transfection of the HCC827GR cells with miR-NC and miR-625-3p, RNA was extracted to examine miR-625-3p and *AXL* expression to confirm whether miR-625-3p was upregulated and *AXL* was downregulated in the cells. We also extracted RNA from HCC827GR cells transfected with si-NC and si-*AXL* to confirm whether *AXL* was downregulated.

Reverse transcription was performed using reverse transcriptase M-MLV (Takara) according to the manufacturer's protocol. miR-625-3p and U6-specific cDNA were synthesized using gene-specific primers designed and synthesized by Guangzhou RiboBio Co. (cat. no. MQPS0001992-1-100 and MQPS0001992-1-100). Reverse transcription polymerase chain reaction (RT-qPCR) was performed using SYBR Premix ExTaq™ (Takara) according to the manufacturer's instructions. The primer sequences for RT-qPCR of *AXL* and GAPDH were as follows: *AXL* sense, 5'-GGTGGCTGTGAAGACGATGA-3' and antisense, 5'-CTCAGATACTCCATGCCA-3'; GAPDH sense, 5'-TGCACCACCAACTGCTTAGC-3' and antisense, 5'-GGCATGGACTGTGGTCATGG-3'. The PCR programme

was as follows: 50˚C for 2 min; 95˚C for 10 min; and 45 cycles of 95˚C for 15 sec and 60˚C for 1 min. The expression values of *AXL* and miR-625-3p were normalized to the values of the internal controls GAPDH and U6, respectively. Relative expression was calculated using the $2^{-\Delta\Delta Ct}$ method (28).

Western blot analysis. In the present study, HCC827, HCC827GR, HCC82GR cell lines transfected with miR-625-3p, si-*AXL* or negative control were proceeded to extract proteins to identify the changes in the SMAD pathway and EMT-related signaling. Generally, the cells were harvested and lysed on ice for 30 min in RIPA lysis buffer (cat. no. 9806, Cell Signaling Technology, Inc.) to extract protein fractions. The lysates were collected by high-speed centrifugation at 11,000 x g for 15 min at 4˚C. Lysates were subjected to western blot analysis as previously described (29). The antibodies used in our study included anti-vimentin (RV202, dilution 1:1,000, cat. no. 550513, BD Biosciences), anti-pAXL (Y779, dilution 1:1,000, cat. no. AF2228, R&D Systems), and anti-AXL (C89E7, dilution 1:1,000, cat. no. 8661), anti-Smad3 (C67H9, dilution 1:1,000, cat. no. 9523), anti-pSmad3 (Ser423/425, dilution 1:1,000, cat. no. 9520), anti-ZEB1 (D80D3, dilution 1:1,000, cat. no. 3396), anti-Snail (C15D3, dilution 1:1,000, cat. no. 3895s), anti-MMP2 (D8N9Y, dilution 1:1,000, cat. no. 13132), and anti-MMP9 (603H, dilution 1:1,000, cat. no. 13667), anti-N-cadherin (D4R1H, dilution 1:1,000, cat. no. 13116) and anti-E-cadherin (4A2, dilution 1:1,000, cat. no. 14472) (all from Cell Signaling Technology, Inc.), In addition, anti-β-actin (13E5, dilution 1:1,000, cat. no. 4970S) and anti-mouse (dilution 1:2,000, cat. no. 7076S) or anti-rabbit (dilution 1:2,000, cat. no. 7074S) constituted the secondary antibodies and were also purchased from Cell Signaling Technology, Inc.

Statistical analysis. GraphPad Prism 5.02 (GraphPad Software, Inc.) and SPSS 16.0 software (SPSS, Inc.) were used to perform the statistical analysis. Significant differences between two groups were assessed by a non-paired Student's t-test. Significant differences between three groups were analyzed using one-way ANOVA followed by Dunnett's post-hoc test. All statistical tests were two-tailed, and statistical significance was defined as $P<0.05$.

Results

EMT features are detected in HCC827 gefitinib-resistant (HCC827GR) cells without the EGFR T790M mutation. First, we established a gefitinib-resistant subline from the parental HCC827 and PC9 cells harboring EGFR-activating mutations. As shown in Fig. 1A and B, the gefitinib-resistant sublines HCC827GR (IC_{50}: 0.07 μM vs. 23.64 μM) and PC9GR (IC_{50}: 2.06 μM vs. 28.45 μM) manifested significant resistance to gefitinib. The T790M mutation and *MET* gene amplification are the most clearly defined mechanisms underlying acquired resistance to gefitinib. Therefore, we profiled DNA from the cell lines and analyzed the gene status using a capture-based targeted sequencing panel that included the *EGFR* and *MET* genes (Table SI). The results revealed that PC9GR cells acquired a secondary T790M mutation compared with HCC827GR cells, and *MET* gene amplification was not detected (Table SII). Growing evidence has shown that in addition to the T790M mutation and *MET* amplification, EMT plays an important role in acquired resistance to EGFR-TKIs. EMT is an important process during malignant cancer progression, accompanied by upregulation of N-cadherin and vimentin and downregulation of E-cadherin (30). Furthermore, wound healing and Transwell assays were performed, and the results showed that HCC827GR cells contained high migratory and invasive ability compared with HCC827 cells (Fig. 1C and D). Moreover, western blot analysis revealed decreased protein levels of E-cadherin and increased protein levels of N-cadherin and vimentin in the HCC827GR cells (Fig. 1E).

miR-625-3p is decreased in HCC827GR cells, and overexpression of miR-625-3p attenuates gefitinib resistance via regulation of EMT phenotypes. MicroRNAs can regulate multiple signaling cascades via transcriptional silencing effects. First, microRNA library construction and RNA sequencing were performed. We found 16 upregulated microRNAs and 27 downregulated microRNAs in HCC827GR cells when compared to the parental cells [Fig. 2A, >1.5-fold change, false discovery rate (FDR) <0.05, $P<0.05$]. To verify the results above, we performed RT-qPCR analysis and found that miR-625-3p expression was significantly reduced in HCC827GR cells compared with HCC827 cells (Fig. 2B, $P<0.001$). In addition, data showed similar downregulated miR-625-3p expression in PC9GR cells when compared to PC9 cells (Fig. S1A).

As microRNA interventions can attenuate EGFR-TKI-resistant phenotypes, we next verified whether miR-625-3p overexpression could reverse the acquired resistance to EGFR-TKI. HCC827GR cells were transfected with miR-625-3p mimics (Fig. 3A). As shown in Fig. 3B, our results demonstrated that overexpression of miR-625-3p could partly reverse gefitinib resistance in the HCC827GR cells. In addition, the IC_{50} value declined to 12.26 μM after miR-625-3p transfection. Considering the findings that EMT is a mechanism of acquired resistance to EGFR-TKI, wound healing and Transwell assays were performed. The results showed that overexpression of miR-625-3p inhibited the migratory and invasive ability of the HCC827GR cells (Fig. 3C and D). Moreover, western blot analysis showed increased E-cadherin expression and decreased N-cadherin and vimentin expression after miR-625-3p overexpression (Fig. 3E).

AXL is upregulated in EGFR-TKI-resistant lung cancer cell lines and is a direct target of miR-625-3p. It is well accepted that microRNAs execute their function by attenuating the stability and translation of downstream target genes. The miRanda and RNAhybrid databases were used to predict the potential mRNAs targeted by miR-625-3p. Among all mRNAs presented in Fig. 4A, *AXL* has been shown to be associated with EMT and drug resistance (31,32). Therefore, we focused on *AXL* as a new post-transcriptional mechanism of miR-625-3p. RNA sequencing showed that *AXL* was upregulated in the HCC827GR cells (Fig. 4B). Additionally, upregulated *AXL* expression was also found in HCC827 erlotinib-resistant cells based on the data extracted from the public datasets GSE38121 and GSE71587 (Fig. 4C and D). To validate that *AXL* is a direct target of miR-625-3p, the *AXL* wild-type (WT) 3'-UTR

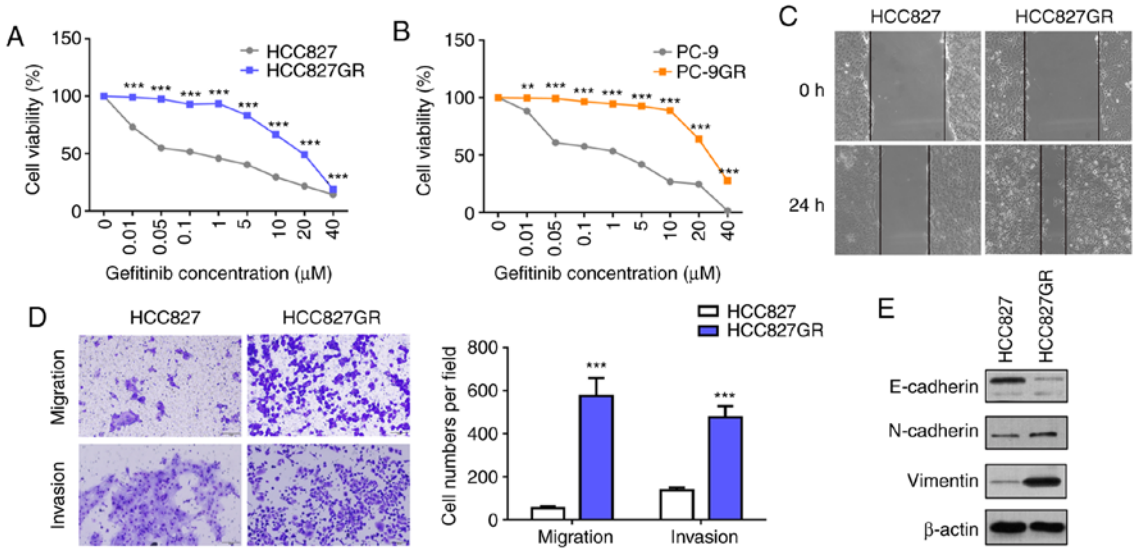

Figure 1. EMT features are detected in HCC827GR cells without the T790M mutation. (A and B) Construction of the gefitinib-resistant HCC827GR and PC9GR cell lines. (C) A wound healing assay was performed in the HCC827 and HCC827GR cell lines (magnification, x100). (D) Migration and invasion assays in the HCC827 and HCC827GR cell lines. (E) Western blot analysis of E-cadherin, N-cadherin and vimentin expression in HCC827GR cells compared to HCC827 cells. **P<0.01, ***P<0.001, parental cell line compared to the gefitinib-resistant cell line. EMT, epithelial to mesenchymal transition.

(containing the miR-625-3p binding sequence) and the *AXL* MUT 3'-UTR were constructed (Fig. 5A). The dual-luciferase reporter assay conducted in 293T cells showed that miR-625-3p significantly inhibited the luciferase activity in cells transfected with the wild-type *AXL* 3'-UTR but did not in cells transfected with the mutant construct (Fig. 5B). Moreover, we also performed the luciferase assay in HCC827 and HCC827GR cells and got similar results (Fig. S2). In addition, we found that *AXL* expression was downregulated in the HCC827GR cells at both the mRNA and protein levels after transfection with miR-625-3p mimics (Fig. 5C and D). Collectively, our data showed that *AXL* is a target of miR-625-3p in NSCLC cells.

AXL knockdown attenuates gefitinib resistance in HCC827GR cells by reversing EMT phenotypes. The role of *AXL*-mediated EMT and drug resistance has been documented in many types of cancers, especially lung cancer. First, we performed RT-qPCR analysis to confirm the results from RNA sequencing and found that the *AXL* level was significantly increased in HCC827GR cells compared with that noted in the HCC827 cells (Fig. 6A, P<0.01). In contrary, PC9GR cells were found to contain lower *AXL* mRNA expression when compared to PC9 cells (Fig. S1B). Next, we inhibited *AXL* using specific small interfering RNA (siRNA) and found that knockdown of *AXL* enhanced gefitinib sensitivity in the HCC827GR cells. Similarly, the IC_{50} value decreased to 18.02 μM after *AXL* knockdown (Fig. 6B and C). To investigate whether knockdown of *AXL* enhanced gefitinib sensitivity by reversing EMT, wound healing and Transwell assays were performed. The results showed that *AXL* knockdown significantly inhibited the migratory and invasive ability of HCC827GR cells (Fig. 6D and E). Western blot analysis demonstrated increased protein levels of E-cadherin and decreased protein levels of N-cadherin and vimentin in the HCC827GR cells following *AXL* knockdown (Fig. 6F).

miR-625-3p/AXL axis contributes to gefitinib resistance via the SMAD pathway. From previous results we know that overexpression of miR-625-3p or knockdown of *AXL* can attenuate gefitinib resistance by reversing the EMT phenotype. However, the underlying mechanism remains unclear. Given that the transforming growth factor (TGF)-β1 signaling pathway can contribute to the EMT phenotype in the progression of various cancers (33,34), and that Smad3 functions as a canonical downstream player involved in the TGF-β1 signaling pathway (35,36), we hypothesized that Smad3 may participate in *AXL*-mediated acquired resistance to gefitinib. As shown in Fig. 7A, western blot analysis demonstrated that the expression level of phosphorylated Smad3 was increased in the HCC827GR cell line compared to that found in the HCC827 cells. In addition, the expression of the transcription factors Snail and ZEB1 was increased in the HCC827GR cells. MMP family members, such as MMP2 and MMP9, showed similar upregulated tendencies. Moreover, knockdown of *AXL* and overexpression of miR-635-3p decreased the protein levels of p-Smad3, ZEB1, Snail, MMP2 and MMP9 in the HCC827GR cells. All these changes confirmed that the TGF-β1/Smad3 pathway was indeed involved in the miR-625-3p/*AXL* axis-mediated gefitinib resistance (Fig. 7A).

Discussion

Recently, the identification of epidermal growth factor receptor (*EGFR*) mutations as oncogenic drivers has launched the era of precision medicine in the treatment of non-small cell lung cancer (NSCLC). A majority of patients who carry *EGFR*-sensitive mutations, such as exon 19 deletions (del 19) and exon 21 L858R substitutions, have benefited from the clinical application of gefitinib (37,38). However, some patients eventually develop acquired drug resistance during treatment, and thus, the efficacy is limited. It has been reported that the T790M mutation accounts for more than 50% of the

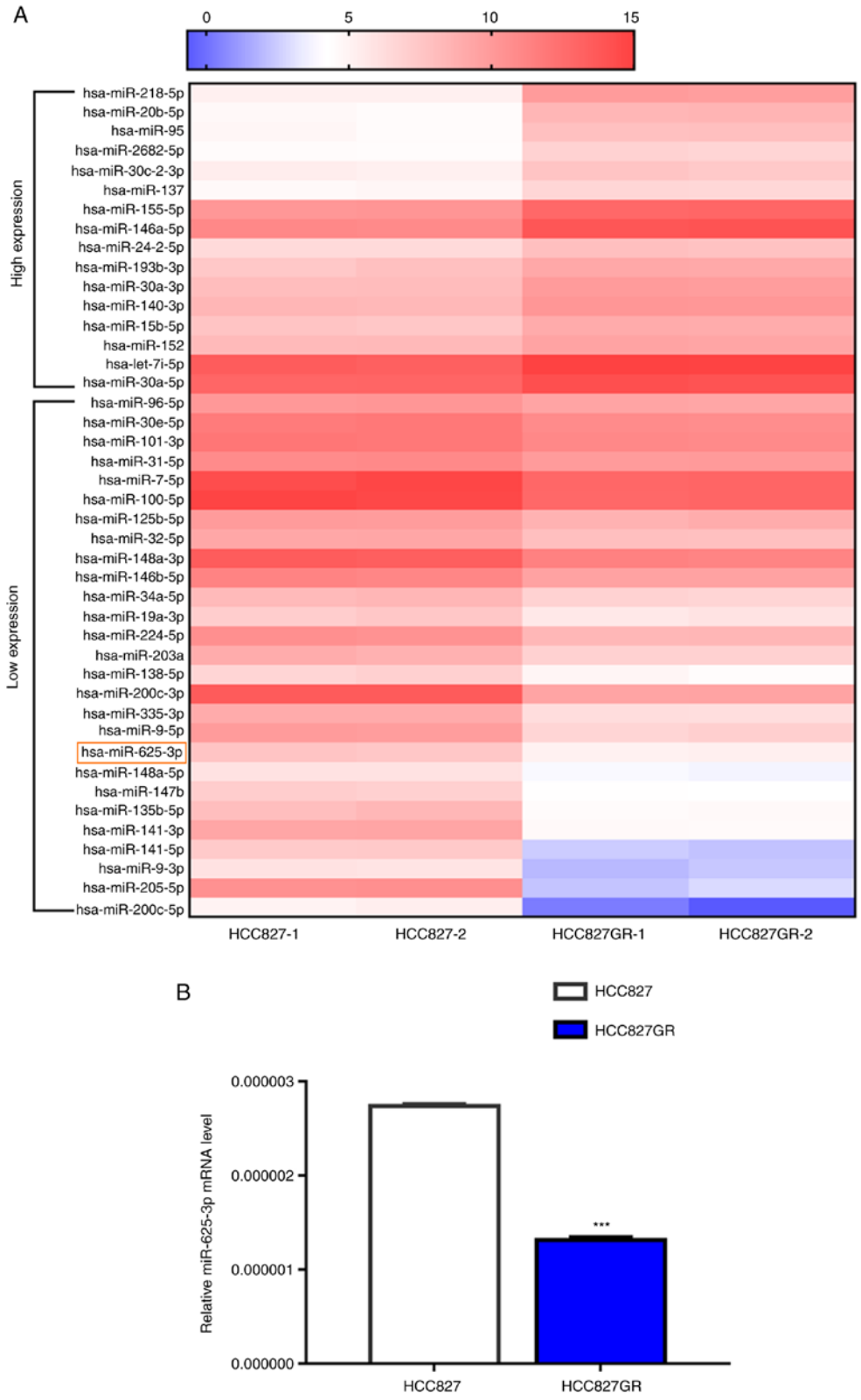

Figure 2. miR-625-3p is significantly downregulated in gefitinib-resistant HCC827GR cells. (A) MicroRNA library construction and RNA sequencing were performed. A total of 16 microRNAs were upregulated and 27 microRNAs were downregulated. (B) Among all downregulated microRNAs, miR-625-3p was significantly downregulated in HCC827GR cells compared to HCC827 cells. ***P<0.001.

cases of known acquired resistance. However, the mechanism for acquired resistance in the remaining patients without the T790M mutation still needs to be explored. After profiling DNA from cell lines using a capture-based targeted sequencing panel, we found that PC9GR cells contained the T790M mutation compared to HCC827GR cells. Therefore, in the next step, we mainly focused on the mechanism of resistance to gefitinib in the HCC827GR cell line.

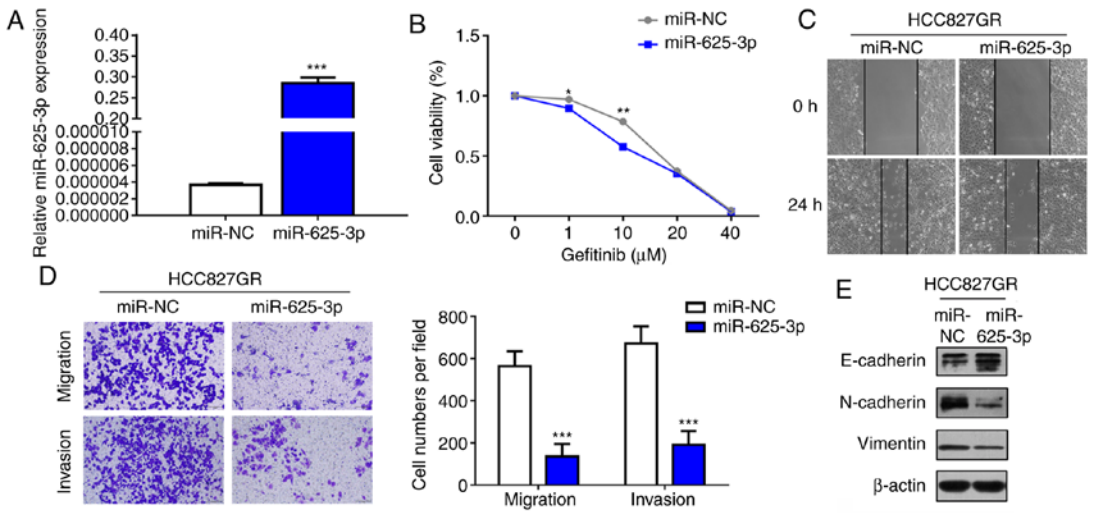

Figure 3. Overexpression of miR-625-3p attenuates gefitinib resistance by regulating EMT phenotypes. (A) RT-qPCR analysis of miR-625-3p expression in HCC827GR cells after transfection with miR-625-3p mimic. (B) The viability of gefitinib-resistant HCC827GR cells after transfection with miR-625-3p mimics and then treatment with gefitinib. (C) After transfection with miR-625-3p mimics, the wound healing assay was performed in HCC827GR cells, and miR-NC was used as a control (magnification, x100). (D) Transwell assays in HCC827GR cells after transfection with miR-625-3p mimics or miR-NC. (E) Western blot analysis of N-cadherin, E-cadherin and vimentin expression in HCC827GR cells after transfection with miR-625-3p. *P<0.05, **P<0.01, ***P<0.001, compared to the miR-NC group. EMT, epithelial to mesenchymal transition; NC, negative control.

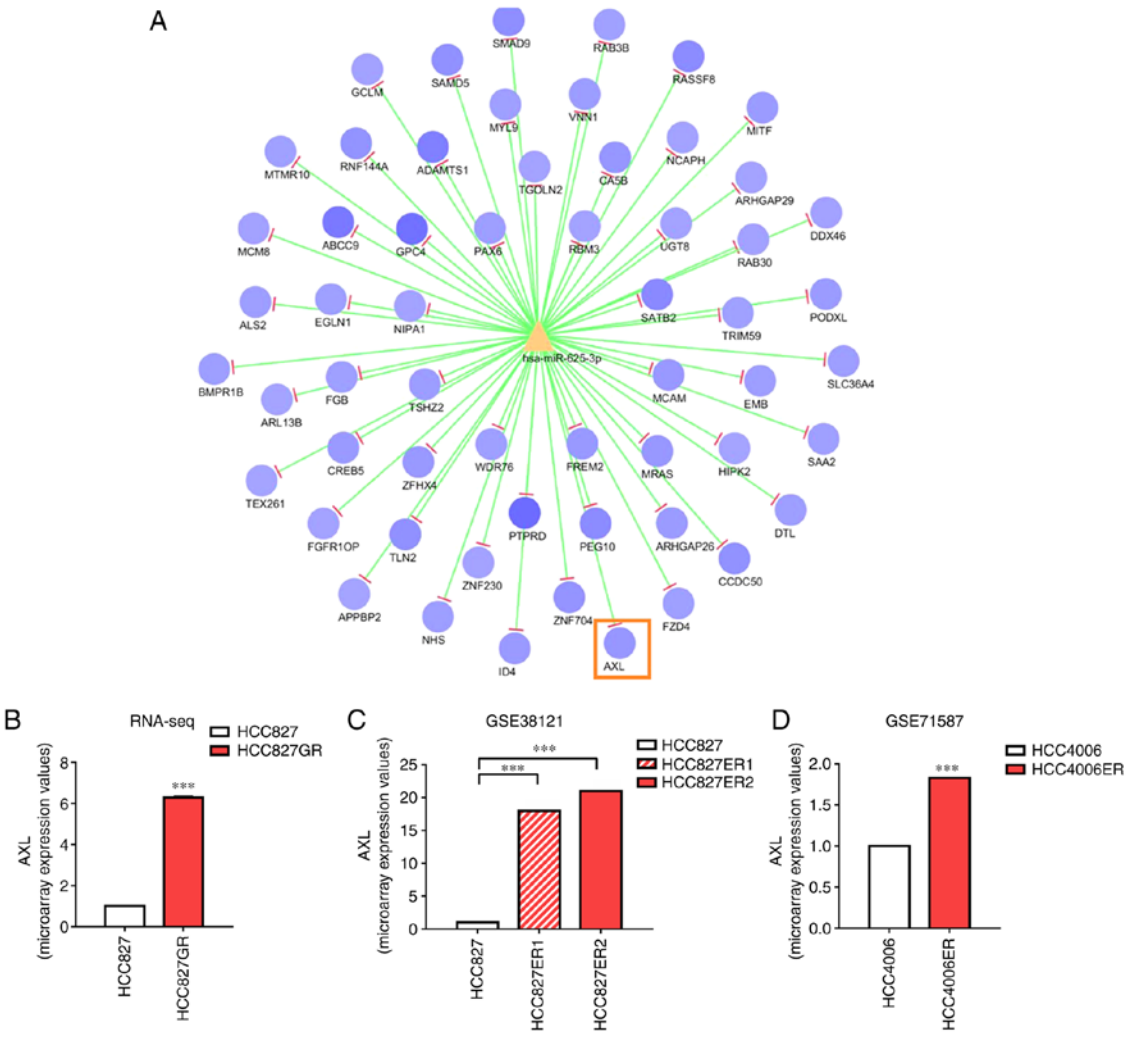

Figure 4. *AXL* is highly expressed in drug-resistant cells. (A) RNA sequencing showed that *AXL* is a potential target of miR-625-3p. (B) *AXL* is overexpressed in gefitinib-resistant HCC827GR cells based on RNA sequencing data. (C) The GSE38121 dataset showed that *AXL* is highly upregulated in erlotinib-resistant HCC827ER cells. (D) The GSE71587 dataset showed higher expression of *AXL* in erlotinib-resistant HCC4006ER cells. ***P<0.001, compared to parental cell line. *AXL*, AXL receptor tyrosine kinase.

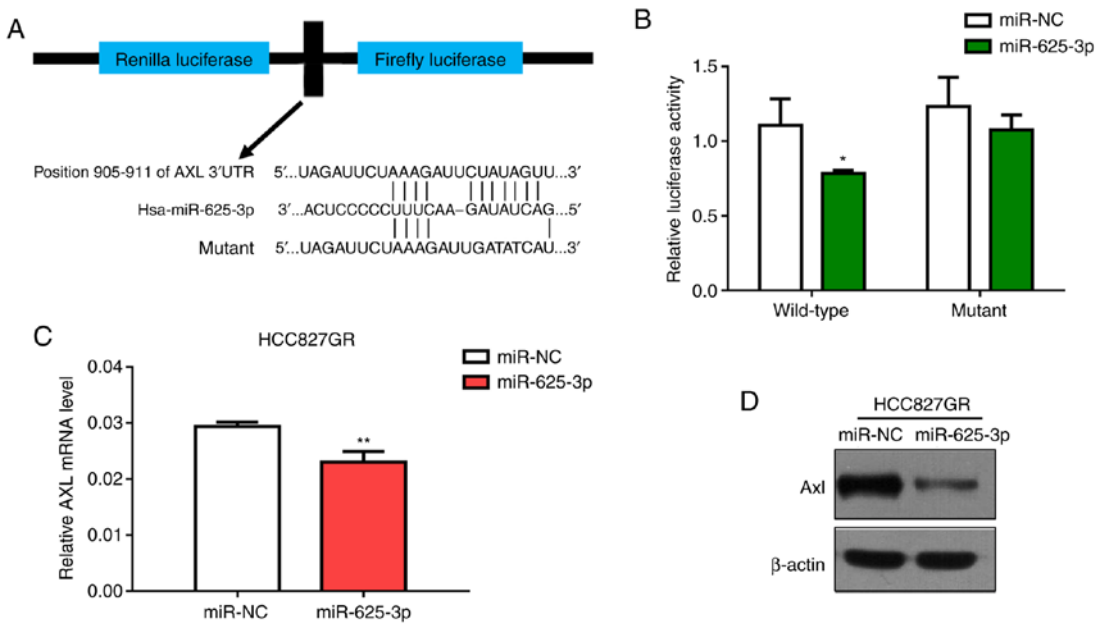

Figure 5. *AXL* is a direct target of miR-625-3p. (A) Schematic construction of the psiCHECK-2 luciferase reporter containing the predicted miR-625-3p binding sites (position 905-911) or the mutant sites located in the 3'-UTR of *AXL*. (B) Luciferase activity in 293T cells after co-transfection of the construct containing the wild-type or mutant *AXL* 3'-UTR reporter gene and the miR-625-3p mimics or miR-NC. (C and D) RT-qPCR and western blot analysis of *AXL* expression after transfection with miR-625-3p mimic. **P<0.01. *AXL*, AXL receptor tyrosine kinase; UTR, untranslated region; NC, negative control.

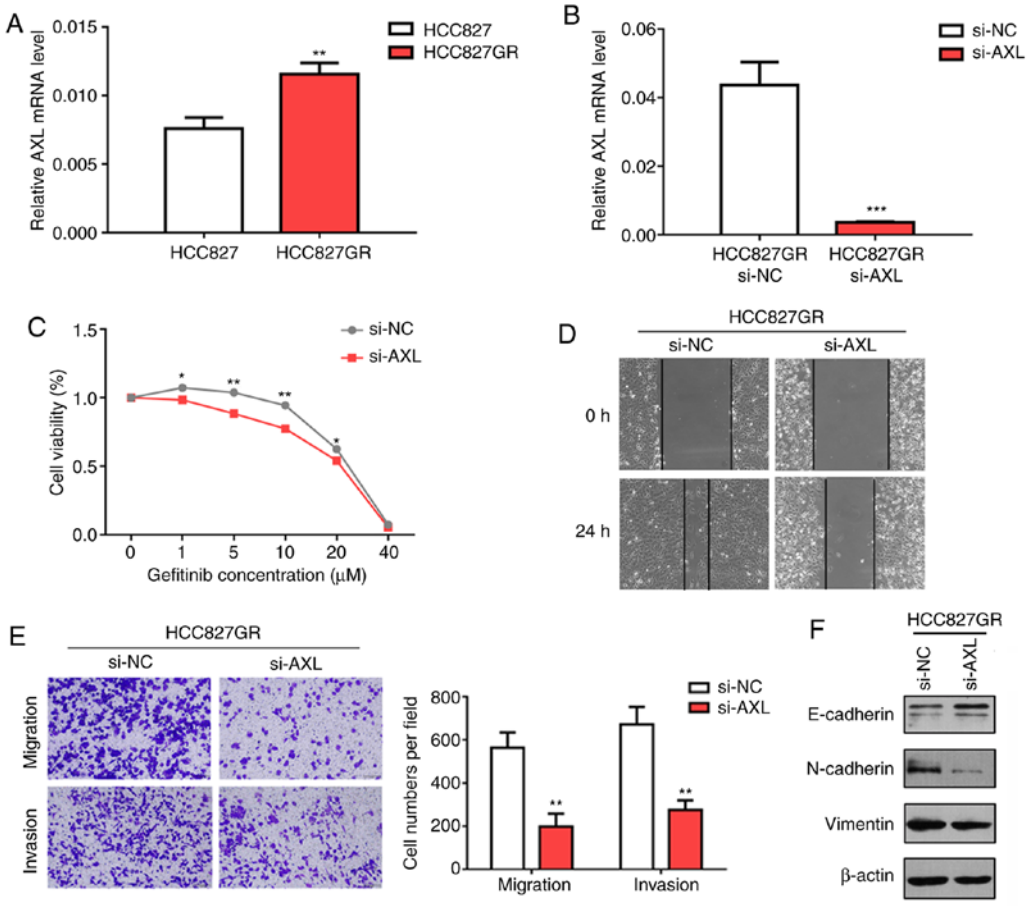

Figure 6. *AXL* knockdown attenuates gefitinib resistance in gefitinib-resistant HCC827GR cells by reversing EMT phenotypes. (A) *AXL* is highly expressed in HCC827GR cells compared to HCC827 cells. (B) RT-qPCR analysis of *AXL* expression in HCC827GR cells after knockdown of *AXL*. (C) The viability of HCC827GR cells after knockdown of *AXL* and treatment with gefitinib. (D) The wound healing assay in HCC827GR cells after knockdown of *AXL* expression (magnification, x100). (E) The Transwell assay in HCC827GR cells after knockdown of *AXL* expression. (F) Western blot analysis of E-cadherin, N-cadherin and vimentin expression in HCC827GR cells after knockdown of *AXL* expression. *P<0.05, **P<0.01, ***P<0.001, compared with the si-NC group. *AXL*, AXL receptor tyrosine kinase; EMT, epithelial to mesenchymal transition; si-NC, negative control siRNA; si-AXL, *AXL* siRNA.

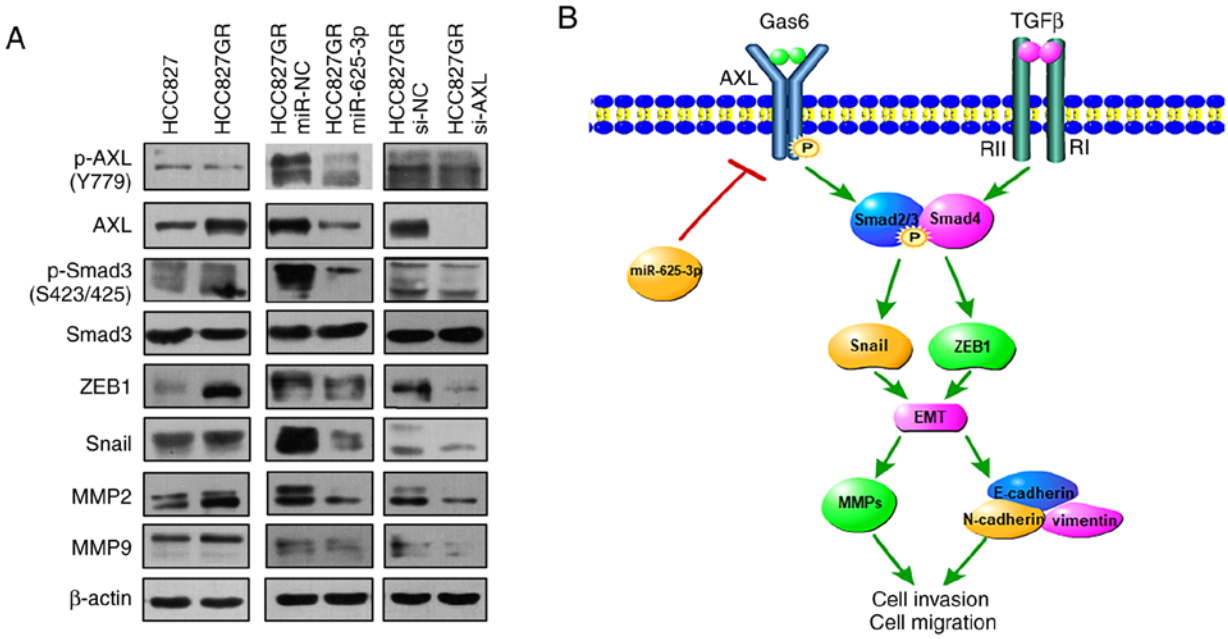

Figure 7. The miR-625-3p/*AXL* axis contributes to gefitinib resistance via the SMAD pathway. (A) Western blot analysis of *AXL*, phosphorylated (p)-*AXL*, Smad3, p-Smad3, ZEB1, Snail, MMP2, and MMP9 expression in the parental HCC827GR cells compared to HCC827 cells or in cells after transfection of miR-625-3p mimic or knockdown of *AXL*. (B) A diagram of the mechanism of miR-625-3p/*AXL*-mediated gefitinib resistance. Gas6, growth arrest specific 6; TGFβ, transforming growth factor β; *AXL*, AXL receptor tyrosine kinase;; ZEB1, zinc finger E-box binding homeobox 1; MMP, matrix metalloproteinases; Snail, Snail family transcriptional repressor 1; p, phorphorylation; EMT, epithelial to mesenchymal transition.

MicroRNAs are important regulators in tumor development and progression. A vast variety of evidence also indicates that microRNAs can participate in the acquired resistance to epidermal growth factor receptor-tyrosine kinase inhibitors (EGFR-TKIs). It has been reported that microRNA-147 overexpression can induce colon cancer cells to undergo a mesenchymal-to-epithelial transition phenotype to reverse gefitinib resistance (39). In NSCLC, miR-124 modulates gefitinib resistance through *SNAI2* and *STAT3*, providing a therapeutic strategy for reversing acquired gefitinib resistance in patients (40). Our microarray data showed that miR-625-3p was significantly downregulated in HCC827GR cells compared to HCC827 cells, implying that miR-625-5p may play an important role in the development of resistance to EGFR-TKIs.

Importantly, we found that overexpression of miR-625-3p decreased the IC_{50} value in HCC827GR cells and thus partly reversed gefitinib resistance. The EMT process has been demonstrated to contribute to acquired resistance to gefitinib. Consequently, next we mainly focused on whether overexpression of miR-625-5p could induce mesenchymal-to-epithelial transition to reverse gefitinib resistance. The Transwell and wound healing assays both showed that overexpression of miR-625-3p inhibited the migratory and invasive ability of HCC827GR cells. Western blot assays further revealed increased expression of E-cadherin and decreased expression of N-cadherin and vimentin in HCC827GR cells transfected with miR-625-3p. All of these findings confirmed that miR-625-3p overexpression indeed induced NSCLC cells to undergo mesenchymal-to-epithelial transition to reverse gefitinib resistance.

After integrating the data obtained from Targetscan analysis, we were surprised to find that AXL receptor tyrosine kinase (*AXL*) was among the potential targets of miR-625-3p. It is known that *AXL* is associated with EMT and TKI resistance. We found higher *AXL* expression in HCC827GR cells based on RNA sequencing analysis. Analysis of data from public databases also demonstrated that *AXL* is highly expressed in both HCC827GR and HCC827 erlotinib-resistant (HCC827ER) cells. Dual-luciferase reporter assays were performed to prove that *AXL* is a direct target of miR-625-3p. After knockdown of *AXL* expression, the IC_{50} value was decreased, and the migratory and invasive ability were decreased in HCC827GR cells. Western blot analysis showed similar results that the expression of E-cadherin was increased. Moreover, the expression of N-cadherin and vimentin were decreased, implying that the cells had acquired a mesenchymal-to-epithelial transition phenotype. We should not ignore the fact that miR-625-3p and AXL mRNA expression were all showed to be downregulated in PC9GR cells when compared to the PC9 cells, indicating that the miR-625-3p/*AXL* axis may be responsible for the mechanism underlying non-T790M mutation. However the hypothesis needs to be further explored.

Tumor growth factor-β1 (TGF-β1)-induced epithelial to mesenchymal transition (EMT) is recognized to contribute to the reduction in drug sensitivity and acquisition of resistance to EGFR-TKIs (41). Among all downstream signaling molecules, the Smad pathway is a major transducer in response to TGF-β1 stimulation. Western blot analysis showed that the expression level of phosphorylated Smad3 was upregulated in the HCC827GR cells. The expression level of p-Smad3 was downregulated after transfection with miR-625-3p or si-*AXL*. In addition to the change in EMT features, ZEB1, Snail, MMP2 and MMP9 levels were also altered. Collectively, these data indicate that the miR-625-3p/*AXL* axis contributes to gefitinib resistance via the SMAD pathway in NSCLC cells.

However, the present study also consisted of various limitations. We did not co-transfect the AXL plasmid and miR-625-3p mimics to assess gefitinib resistance and EMT phenotypes. This rescue experiment can be regarded as another evidence of the miR-625-3p/*AXL* axis. In addition, when we performed the wound healing assay, cells were starved before we scratched the cellular layer. However in various research studies, to prevent cells from proliferating, cells were cultured in serum-free medium or in medium with lower concentrations of FBS after the scratch was made (42,43). Thus, we can repeat the wound healing assay under the latter condition to ensure the accuracy of the results in the future.

In conclusion, this is the first report showing that miR-625-3p overexpression reversed TGF-β1-induced EMT and enhanced gefitinib sensitivity by directly targeting *AXL* in lung cancer cells (Fig. 7B). The miR-625-3p/*AXL* axis was identified as a mechanism for the development of drug resistance in HCC827GR cells without the T790M mutation. Our data may provide therapeutic approaches to increase drug sensitivity and combat resistance to EGFR-TKIs. However, further studies are needed to clarify the underlying mechanism of the miR-625-3p/*AXL* axis and TGF-β1-induced EMT in NSCLC.

Acknowledgements

Not applicable.

Funding

This work was supported by grants from the Jiangsu Provincial Medical Youth Talent (no. QNRC2016746), the Postgraduate Research and Practice Innovation Program of Jiangsu Province (no. KYCX18_2525), the Suzhou Key Laboratory for Respiratory Medicine (no. SZS201617), the Clinical Medical Center of Suzhou (no. Szzx201502), the Jiangsu Provincial Key Medical Discipline (no. ZDXKB2016007), and the National Natural Science Foundation of China (no. 81702870).

Availability of data and materials

The datasets used during the present study are available from the corresponding author upon reasonable request.

Authors' contributions

All authors contributed to this article substantially. WD, LS, and TL performed the experiments. JZ and YZe were responsible for the literature research and collected the cell line data. YZh and XW analysed the data. ZL and JAH contributed to the design of this study and draft of the manuscript. All authors read and approved the manuscript and agree to be accountable for all aspects of the research in ensuring that the accuracy or integrity of any part of the work are appropriately investigated and resolved.

Ethics approval and consent to participate

Not applicable.

Patient consent for publication

Not applicable.

Competing interests

The authors declare that they have no competing interests.

References

1. Siegel RL, Miller KD and Jemal A: Cancer Statistics, 2017. CA Cancer J Clin 67: 7-30, 2017.
2. Yoda S, Dagogo-Jack I and Hata AN: Targeting oncogenic drivers in lung cancer: Recent progress, current challenges and future opportunities. Pharmacol Ther 193: 20-30, 2019.
3. Remon J, Ahn MJ, Girard N, Johnson M, Kim DW, Lopes G, Pillai RN, Solomon B, Villacampa G and Zhou Q: Advanced stage non-small cell lung cancer: Advances in thoracic oncology 2018. J Thorac Oncol 14: 1134-1155, 2019.
4. Zheng L, Wang Y, Xu Z, Yang Q, Zhu G, Liao XY, Chen X, Zhu B, Duan Y and Sun J: Concurrent EGFR-TKI and thoracic radiotherapy as first-line treatment for stage IV non-small cell lung cancer harboring EGFR active mutations. Oncologist 24: e1031-e1612, 2019.
5. Gao J, Li HR, Jin C, Jiang JH and Ding JY: Strategies to overcome acquired resistance to EGFR TKI in the treatment of non-small cell lung cancer. Clin Transl Oncol 21: 1287-1301, 2019.
6. Lee CK, Kim S, Lee JS, Lee JE, Kim SM, Yang IS, Kim HR, Lee JH, Kim S and Cho BC: Next-generation sequencing reveals novel resistance mechanisms and molecular heterogeneity in EGFR-mutant non-small cell lung cancer with acquired resistance to EGFR-TKIs. Lung Cancer 113: 106-114, 2017.
7. Ahsan A: Mechanisms of resistance to EGFR tyrosine kinase inhibitors and therapeutic approaches: An update. Adv Exp Med Biol 893: 137-153, 2016.
8. Zhu X, Chen L, Liu L and Niu X: EMT-mediated acquired EGFR-TKI resistance in NSCLC: Mechanisms and strategies. Front Oncol 9: 1044, 2019.
9. Sato H, Shien K, Tomida S, Okayasu K, Suzawa K, Hashida S, Torigoe H, Watanabe M, Yamamoto H, Soh J, *et al*: Targeting the miR-200c/LIN28B axis in acquired EGFR-TKI resistance non-small cell lung cancer cells harboring EMT features. Sci Rep 7: 40847, 2017.
10. Shah R and Lester JF: Tyrosine kinase inhibitors for the treatment of EGFR mutation-positive non-small-cell lung cancer: A clash of the generations. Clin Lung Cancer: Dec 20, 2019 (Epub ahead of print).
11. Ma Y, Tang N, Thompson RC, Mobley BC, Clark SW, Sarkaria JN and Wang J: InsR/IGF1R pathway mediates resistance to EGFR inhibitors in glioblastoma. Clin Cancer Res 22: 1767-1776, 2016.
12. Wu SG and Shih JY: Management of acquired resistance to EGFR TKI-targeted therapy in advanced non-small cell lung cancer. Mol Cancer 17: 38, 2018.
13. Murtuza A, Bulbul A, Shen JP, Keshavarzian P, Woodward BD, Lopez-Diaz FJ, Lippman SM and Husain H: Novel third-generation EGFR tyrosine kinase inhibitors and strategies to overcome therapeutic resistance in lung cancer. Cancer Res 79: 689-698, 2019.
14. Carlisle JW and Ramalingam SS: Role of osimertinib in the treatment of EGFR-mutation positive non-small-cell lung cancer. Future Oncol 15: 805-816, 2019.
15. Frixa T, Donzelli S and Blandino G: Oncogenic MicroRNAs: Key players in malignant transformation. Cancers (Basel) 7: 2466-2485, 2015.
16. Sin TK, Wang F, Meng F, Wong SC, Cho WC, Siu PM, Chan LW and Yung BY: Implications of MicroRNAs in the treatment of gefitinib-resistant non-small cell lung cancer. Int J Mol Sci 17: 237, 2016.
17. Zang H, Wang W and Fan S: The role of microRNAs in resistance to targeted treatments of non-small cell lung cancer. Cancer Chemother Pharmacol 79: 227-231, 2017.
18. Li B, Ren S, Li X, Wang Y, Garfield D, Zhou S, Chen X, Su C, Chen M, Kuang P, *et al*: MiR-21 overexpression is associated with acquired resistance of EGFR-TKI in non-small cell lung cancer. Lung Cancer 83: 146-153, 2014.

19. Zhu J, Tao L and Jin L: MicroRNA506-3p reverses gefitinib resistance in non-small cell lung cancer by targeting Yes-associated protein 1. Mol Med Rep 19: 1331-1339, 2019.
20. Ma W, Feng W, Tan J, Xu A, Hu Y, Ning L, Kang Y, Wang L and Zhao Z: miR-497 may enhance the sensitivity of non-small cell lung cancer cells to gefitinib through targeting the insulin-like growth factor-1 receptor. J Thorac Dis 10: 5889-5897, 2018.
21. Koizumi F, Shimoyama T, Taguchi F, Saijo N and Nishio K: Establishment of a human non-small cell lung cancer cell line resistant to gefitinib. Int J Cancer 116: 36-44, 2005.
22. Li H and Durbin R: Fast and accurate short read alignment with Burrows-wheeler transform. Bioinformatics 25: 1754-1760, 2009.
23. Kozomara A and Griffiths-Jones S: miRBase: Annotating high confidence microRNAs using deep sequencing data. Nucleic Acids Res 42: D68-D73, 2014.
24. Schneider VA, Graves-Lindsay T, Howe K, Bouk N, Chen HC, Kitts PA, Murphy TD, Pruitt KD, Thibaud-Nissen F, Albracht D, *et al*: Evaluation of GRCh38 and de novo haploid genome assemblies demonstrates the enduring quality of the reference assembly. Genome Res 27: 849-864, 2017.
25. Kim D, Langmead B and Salzberg SL: HISAT: A fast spliced aligner with low memory requirements. Nat Methods 12: 357-360, 2015.
26. Schaid DJ, Sinnwell JP and Thibodeau SN: Robust multipoint identical-by-descent mapping for affected relative pairs. Am J Hum Genet 76: 128-138, 2005.
27. Zhu J, Zeng Y, Xu C, Qin H, Lei Z, Shen D, Liu Z and Huang J: Expression profile analysis of microRNAs and downregulated miR-486-5p and miR-30a-5p in non-small cell lung cancer. Oncol Rep 34: 1779-1786, 2015.
28. Livak KJ and Schmittgen TD: Analysis of relative gene expression data using real-time quantitative PCR and the 2(-Delta Delta C(T)) method. Methods 25: 402-408, 2001.
29. Zhu J, Zeng Y, Li W, Qin H, Lei Z, Shen D, Gu D, Huang JA and Liu Z: CD73/NT5E is a target of miR-30a-5p and plays an important role in the pathogenesis of non-small cell lung cancer. Mol Cancer 16: 34, 2017.
30. Weng CH, Chen LY, Lin YC, Shih JY, Lin YC, Tseng RY, Chiu AC, Yeh YH, Liu C, Lin YT, *et al*: Epithelial-mesenchymal transition (EMT) beyond EGFR mutations per se is a common mechanism for acquired resistance to EGFR TKI. Oncogene 38: 455-468, 2019.
31. Debruyne DN, Bhatnagar N, Sharma B, Luther W, Moore NF, Cheung NK, Gray NS and George RE: ALK inhibitor resistance in ALK(F1174L)-driven neuroblastoma is associated with AXL activation and induction of EMT. Oncogene 35: 3681-3691, 2016.
32. Wu F, Li J, Jang C, Wang J and Xiong J: The role of Axl in drug resistance and epithelial-to-mesenchymal transition of non-small cell lung carcinoma. Int J Clin Exp Pathol 7: 6653-6661, 2014.
33. Lin RL and Zhao LJ: Mechanistic basis and clinical relevance of the role of transforming growth factor-β in cancer. Cancer Biol Med 12: 385-393, 2015.
34. Tan EJ, Olsson AK and Moustakas A: Reprogramming during epithelial to mesenchymal transition under the control of TGFβ. Cell Adhes Migr 9: 233-246, 2015.
35. Jin Q, Gao G and Mulder KM: Requirement of a dynein light chain in TGFbeta/Smad3 signaling. J Cell Physiol 221: 707-715, 2009.
36. Shirai K, Saika S, Tanaka T, Okada Y, Flanders KC, Ooshima A and Ohnishi Y: A new model of anterior subcapsular cataract: Involvement of TGFbeta/Smad signaling. Mol Vis 12: 681-691, 2006.
37. Nukaga S, Yasuda H, Tsuchihara K, Hamamoto J, Masuzawa K, Kawada I, Naoki K, Matsumoto S, Mimaki S, Ikemura S, *et al*: Amplification of EGFR wild-type alleles in non-small cell lung cancer cells confers acquired resistance to mutation-selective EGFR tyrosine kinase inhibitors. Cancer Res 77: 2078-2089, 2017.
38. Corallo S, D'Argento E, Strippoli A, Basso M, Monterisi S, Rossi S, Cassano A and Barone CM: Treatment options for EGFR T790M-negative EGFR tyrosine kinase inhibitor-resistant non-small cell lung cancer. Target Oncol 12: 153-161, 2017.
39. Lee CG, McCarthy S, Gruidl M, Timme C and Yeatman TJ: MicroRNA-147 induces a mesenchymal-to-epithelial transition (MET) and reverses EGFR inhibitor resistance. PLoS One 9: e84597, 2014.
40. Hu FY, Cao XN, Xu QZ, Deng Y, Lai SY, Ma J and Hu JB: miR-124 modulates gefitinib resistance through SNAI2 and STAT3 in non-small cell lung cancer. J Huazhong Univ Sci Technolog Med Sci 36: 839-845, 2016.
41. Kitamura K, Seike M, Okano T, Matsuda K, Miyanaga A, Mizutani H, Noro R, Minegishi Y, Kubota K and Gemma A: MiR-134/487b/655 cluster regulates TGF-β-induced epithelial-mesenchymal transition and drug resistance to gefitinib by targeting MAGI2 in lung adenocarcinoma cells. Mol Cancer Ther 13: 444-453, 2014.
42. Kang CW, Han YE, Kim J, Oh JH, Cho YH and Lee EJ: 4-Hydroxybenzaldehyde accelerates acute wound healing through activation of focal adhesion signalling in keratinocytes. Sci Rep 7: 14192, 2017.
43. Jiang J and Gu J: Beta1,4-galactosyltransferase V A growth regulator in glioma. Methods Enzymol 479: 3-23, 2010.